JOURNAL OF GUIDANCE, CONTROL, AND DYNAMICS
Vol. 19, No. 2, March–April 1996

Extra-Insensitive Input Shapers for Controlling Flexible Spacecraft

William Singhose*
Massachusetts Institute of Technology, Cambridge, Massachusetts 02139
and
Steve Derezinski† and Neil Singer‡
Convolve, Inc., Armonk, New York 10504

A procedure for designing command profiles for flexible spacecraft is presented. The command profiles are required to move a spacecraft from rest to rest or to accelerate a spacecraft to a constant velocity with very little residual vibration. To model the case where the spacecraft is equipped with on-off reaction jets, the command signals are restricted to positive or negative constant-amplitude pulses. The technique results in command profiles that are significantly more robust to modeling errors than profiles developed with similar procedures that have been previously reported. Commands are generated that are much more fuel efficient than profiles obtained with related methods. A technique for eliminating multiple modes of vibration is presented. The control technique is evaluated with both hardware experiments and a highly realistic computer simulation that is used to plan Space Shuttle flights.

Introduction

THE problem of controlling flexible structures in the presence of modeling uncertainties and structural nonlinearities is an area of active research. The techniques currently under investigation include adding damping to the system, stiffening the structure, developing a sophisticated model and controller, and shaping the command signals. For space-based systems, the first two options can be suboptimal because they usually require additional mass. The third option is application specific and developments may be difficult to generalize. Generating command signals that do not excite unwanted dynamics is often the most appealing option.

The technique of input shaping to control flexible structures has received much attention during the past few years. Input shaping is implemented by convolving a sequence of impulses, an input shaper, with a desired system command to produce a shaped input that is then used to drive the system.[1] The input shaper is determined from a set of equations that constrain the dynamic performance of the system. In general, the input shaping process leads to a variable-amplitude command signal.

Input shaping has been investigated and extended by many researchers since the original presentation in Ref. 1. Singhose et al.[2,3] proposed a technique for improving insensitivity to modeling errors and parameter variations. Hyde and Seering[4] demonstrated that the input-shaping process generates time-optimal inputs for multiple-mode systems. Banerjee[5] used input shaping to reduce residual vibration and maximum deflections during the simulation of a large space-based antenna. Rappole et al.[6] used two-mode input shapers to increase the throughput of a wafer handling robot. Jansen[7] and Magee and Book[8] used input shaping on long-reach manipulators. Tzes and Yurkovich[9] used input shaping in an adaptive controller. Murphy and Watanabe[10] took into account the effect of coarse digitization on input shaping.[10]

Several researchers have presented methods for designing-input shapers in the z plane.[11–13] Input shapers containing negative impulses were shown to improve response time.[14,15] Input shaping was shown to be beneficial for trajectory following.[16,17]

Flexible spacecraft equipped with on-off reaction jets cannot produce the variable-amplitude actuation force that is usually required with input shaping; the spacecraft must be moved with constant-amplitude force pulses. Some approximate methods for extending input shaping to the case where only constant-amplitude pulses are available have been developed.[18,19] The patented method of input shaping[20] can be applied to the problem of controlling flexible spacecraft equipped with on-off reaction jets by adding a constraint on actuator effort. The set of constraint equations can be solved with a standard optimization package. Liu and Wie,[21] Singh and Vadali,[22] and Wie et al.[23] demonstrated their results with a two-mass spring and damper simulation. Banerjee[5] and Banerjee and Singhose[24] demonstrated the utility of the approach with a nonlinear simulation of the Waves In Space Plasma antenna.

This paper presents a new procedure for designing input shapers for use with on-off reaction jets. The command profiles obtained with the new procedure are significantly more robust to modeling errors than the shaped command profiles previously reported in references.[5,21,22] The algorithm we present can be extended to accommodate any range of frequency errors. Furthermore, command profiles are developed that are much more fuel efficient than those previously reported. Finally, the procedure can be used to eliminate multiple modes of vibration.

The simple model used previously in the literature[21,22] will be used to compare our results with those previously reported. The method will then be rigorously tested using Draper Laboratory's simulation of the Space Shuttle's remote manipulator. This simulation is used to plan maneuvers during Space Shuttle flights. Hardware results from a flexible system equipped with on-off actuators will also be presented as a demonstration of the multimode capabilities.

Development of Constraint Equations

One of the great advantages of input shaping is that it requires only a simple system model like the one shown in Fig. 1. Simple models can be used because the equations used to reduce the residual vibration only contain the natural frequencies and damping ratios of the system. Furthermore, input shaping can be made robust to modeling errors, which allows the command profiles developed for simple systems to work effectively on more complex systems.

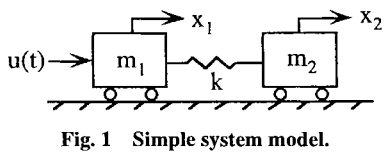

Fig. 1 Simple system model.

Received June 10, 1995; revision received Sept. 1, 1995; accepted for publication Sept. 5, 1995.

*Research Assistant, Department of Mechanical Engineering. Member AIAA.
†Mechanical Engineer.
‡President.

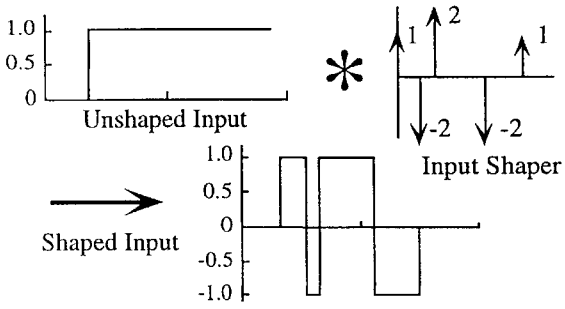

Fig. 2 Input shaping to generate a series of alternating-sign pulses.

The model shown in Fig. 1 represents a system with a single flexible mode and a rigid-body mode. A force input $u(t)$ acts on mass m_1 and is restricted to have a value of $+1$, 0, or -1. We have left out damping to simplify the examples; however, the technique can be used with damped systems by simply adding damping terms in the constraint equations.[22]

A set of constraint equations based on the simple model is formulated so that even a physically complex system responds with very little residual vibration. Additional equations can be used to cancel multiple modes, accommodate actuator limits, and control move distance and velocity. By solving the system of constraint equations, the amplitudes and time locations of the input shaper impulses can be determined.

The inputs to the system under consideration must consist only of positive or negative constant-amplitude force pulses. For rest-to-rest slews, the commands must contain both positive and negative pulses so that the system can be accelerated and then decelerated back to zero velocity. A series of alternating-sign pulses for rest-to-rest slews can be generated by convolving a step with an input shaper of the form

$$\begin{bmatrix} A_i \\ t_i \end{bmatrix} = \begin{bmatrix} 1 & -2 & 2 & -2 & \cdots & -2 & 1 \\ 0 & t_2 & t_3 & t_4 & \cdots & t_{n-1} & t_n \end{bmatrix} \tag{1}$$

where $i = 1, \ldots, n$, A_i is the amplitude of the ith impulse, t_i is the time location of the ith impulse, and n is odd. Figure 2 demonstrates that a step convolved with this type of an input shaper results in a series of alternating sign, variable-width pulses. Equation (1) leads to our first constraint equations for rest-to-rest shapers:

$$\begin{aligned} A_i &= 1 \qquad && i = 1, n \\ A_i &= 2(-1)^{i-1} \qquad && i = 2, \ldots, n-1 \end{aligned} \tag{2}$$

For maneuvers that spin up to a constant velocity, the command can consist of a series of alternating pulses or a series of only positive pulses. The fastest spin-up maneuver requires both positive and negative force pulses.[22] Unfortunately, the negative force pulses lead to poor fuel efficiency. Therefore, we will develop spin-up commands that use only positive pulses. Using only positive pulses increases the maneuver time only slightly.[25] To generate a series of positive pulses, an input shaper must have the form

$$\begin{bmatrix} A_i \\ t_i \end{bmatrix} = \begin{bmatrix} 1 & -1 & 1 & \cdots & 1 & -1 \\ 0 & t_2 & t_3 & \cdots & t_{m-1} & t_m \end{bmatrix} \tag{3}$$

where m is an even integer. Equation (3) leads to a constraint equation on the positive-pulse shaper amplitudes:

$$A_i = (-1)^{i-1} \qquad i = 1, \ldots, m \tag{4}$$

The next constraint equations ensure that the system's mass center will move the desired amount. The rigid-body motion can be described as

$$\ddot{x} = \frac{u(t)}{(m_1 + m_2)} \tag{5}$$

where x is the displacement of the mass center. By integrating Eq. (5) with respect to time we get a constraint on mass center velocity:

$$v_d = \int \frac{u(t)}{(m_1 + m_2)}\,\mathrm{d}t \tag{6}$$

where v_d is the desired velocity. Integrating once more gives a constraint on move distance:

$$x_d = \iint \frac{u(t)}{(m_1 + m_2)}\,\mathrm{d}t\,\mathrm{d}t \tag{7}$$

where x_d is the desired move distance.

The rigid-body motion is set by Eqs. (6) and (7); however, the main purpose of input shaping is to limit the amount of residual vibration that occurs when the system reaches its desired setpoint. The constraint equation limiting vibration amplitude can be formulated as a ratio of residual vibration amplitude with input shaping divided by residual vibration without shaping. By forming the constraint equation as a ratio, the amount of residual vibration can be specified as a percentage of the vibration that would occur without input shaping.

To construct the vibration ratio equation and select a benchmark to measure performance, we must assume a form for the unshaped input. Because the techniques in this paper are designed for use with on-off actuators, it would be appropriate to use a baseline input that is either a bang-bang or a single pulse in force. Whenever possible the bang-bang input is used as the standard for commands that slew from rest to rest and the single pulse is the baseline for commands that accelerate to a constant velocity.

On occasion it is not feasible to form the ratio equation relative to a bang-bang or a pulse. The problem arises when the residual vibration from the baseline input goes to zero. This, of course, makes the ratio go to infinity. The vibration from a bang-bang or pulse input will be zero when the width of the pulses is equal to the period of system vibration. When the ratio cannot be formed relative to the baseline commands, the ratio will be formed relative to a step input. (The residual vibration from a step input is never zero for undamped or lightly damped systems.)

A bang-bang input can be viewed as a step input convolved with a shaper of the form

$$\begin{bmatrix} A_j \\ t_j \end{bmatrix} = \begin{bmatrix} 1 & -2 & 1 \\ 0 & t_{bbs} & t_{bbl} \end{bmatrix} \tag{8}$$

where t_{bbs} is the switching time and t_{bbl} is the length of the bang-bang. This is demonstrated by the first three impulses in Fig. 2 if the value of the third impulse is changed from 2 to 1.

A single pulse can be viewed as a step input convolved with a two-impulse shaper of the form

$$\begin{bmatrix} A_i \\ t_i \end{bmatrix} = \begin{bmatrix} 1 & -1 \\ 0 & t_p \end{bmatrix} \tag{9}$$

where t_p is the length of the pulse.

The amplitude of residual vibration of an undamped second-order system when subjected to a sequence of impulses can be expressed as a summation of the responses to individual impulses that is given in the references.[26] The expression giving the amplitude is

$$R_{\text{amp}} = \sqrt{[\Sigma A_i \sin(\omega t_i)]^2 + [\Sigma A_i \cos(\omega t_i)]^2} \tag{10}$$

where ω is the undamped natural frequency. We can construct the ratio of shaped to unshaped vibration by dividing Eq. (10) for the input shaper by the equivalent Eq. (10) for the impulse sequence corresponding to the unshaped input. The percentage vibration relative to a bang-bang is

$$V = \sqrt{\frac{[\Sigma A_i \sin(\omega t_i)]^2 + [\Sigma A_i \cos(\omega t_i)]^2}{[\Sigma A_{BBj} \sin(\omega t_{BBj})]^2 + [\Sigma A_{BBj} \cos(\omega t_{BBj})]^2}} \tag{11}$$

where A_{BBj} and t_{BBj} describe the input shaper corresponding to the bang-bang and are given by Eq. (8).

The percentage vibration relative to a pulse is

$$V = \sqrt{\frac{[\Sigma A_i \sin(\omega t_i)]^2 + [\Sigma A_i \cos(\omega t_i)]^2}{[\Sigma A_{Pi} \sin(\omega t_{Pi})]^2 + [\Sigma A_{Pi} \cos(\omega t_{Pi})]^2}} \tag{12}$$

where A_{Pi} and t_{Pi} are the amplitudes and time locations of the input shaper corresponding to the pulse [Eq. (9)].

By including Eq. (11) or (12) in our set of constraint equations, we can set the level of vibration to the quantity V when the system's frequency is exactly ω. For example, when $V = 0.05$, the shaped vibration amplitude is 5% of the baseline vibration amplitude. However, if the frequency varies from ω, then there may exist a large amount of residual vibration. An effective procedure for making the vibration reduction robust to modeling errors was first suggested in Ref. 1. The procedure requires taking the derivative of the residual vibration equation with respect to the frequency and setting the result equal to zero. When this is done the amplitude of residual vibration will change very little if the frequency differs from its modeled value. Consequently, the residual vibration amplitude stays close to the small value V as the frequency shifts away from the modeling frequency. When the residual vibration is expressed in terms of the bang-bang ratio, the derivative constraint is

$$\frac{d}{d\omega}\sqrt{\frac{[\Sigma A_i \sin(\omega t_i)]^2 + [\Sigma A_i \cos(\omega t_i)]^2}{[\Sigma A_{BBj} \sin(\omega t_{BBj})]^2 + [\Sigma A_{BBj} \cos(\omega t_{BBj})]^2}} = 0 \qquad (13)$$

For the pulse ratio, the constraint is

$$\frac{d}{d\omega}\sqrt{\frac{[\Sigma A_i \sin(\omega t_i)]^2 + [\Sigma A_i \cos(\omega t_i)]^2}{[\Sigma A_{Pi} \sin(\omega t_{Pi})]^2 + [\Sigma A_{Pi} \cos(\omega t_{Pi})]^2}} = 0 \qquad (14)$$

The final constraint ensures that our solution is time optimal; that is, it is the shortest command signal that meets the other constraints. The constraint is simply

$$\text{minimize } (t_n) \qquad (15)$$

where t_n is the time of the last shaper impulse.

Equations (2), (7), (11), (13), and (15) form the set of constraint equations we will use to design rest-to-rest input shapers. Equations (4), (6), (12), (14), and (15) form the set of constraint equations we will use to design input shapers for accelerating a flexible spacecraft to constant velocity.

Input Shaper Design for Rest-to-Rest Slews

In this section, a new type of rest-to-rest input shaper will be designed using the constraint equations of the previous section. The performance of the new shaper will be compared with results presented in the references.[21,22]

The extra-insensitive (EI) input shaper is designed by setting V to a nonzero value in Eq. (11). Two more constraint equations are obtained by setting Eq. (11) equal to zero at two other frequencies, one higher than the modeling frequency, ω_{hi}, and the other lower, ω_{lo}. The values of the frequencies ω_{hi} and ω_{lo} are not specified; they are variables that depend on the value of V. We also require the derivative of the percentage vibration [Eq. (13)] to be zero at the modeling frequency. When the set of constraint equations is solved with an optimization program such as GAMS,[27] the values of the impulse time locations, as well as ω_{hi} and ω_{lo}, are determined. When the EI constraints are solved for the model shown in Fig. 1 with parameter values of $V = 0.05$ and $m_1 = m_2 = k = x_d = 1$, the resulting input shaper is

$$\begin{bmatrix} A_i \\ T_i \end{bmatrix} = \begin{bmatrix} 1 & -2 & 2 & -2 & 2 & -2 & 1 \\ 0 & 0.7286 & 1.6921 & 2.951 & 4.2098 & 5.1733 & 5.9019 \end{bmatrix} \qquad (16)$$

The input shapers presented previously in the literature required the residual vibration to exactly equal zero (instead of V) when the system model is exact. Although this robustness constraint is reasonable (it is the constraint used in the original formulation of input shaping), it can be seen to be an excessive constraint. The primary reason for input shaping is to eliminate vibration in the presence of modeling errors. In other words, the control engineer

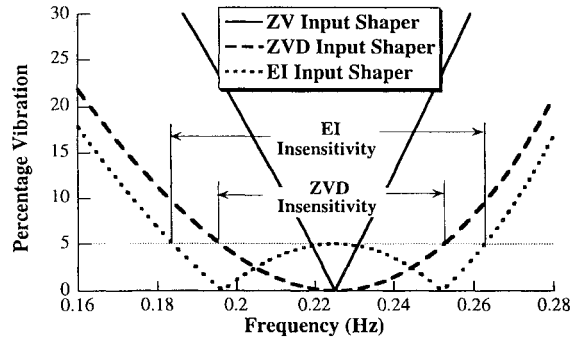

Fig. 3 Sensitivity curves for the ZV, ZVD, and EI rest-to-rest shapers ($m_1 = m_2 = k = x_d = 1$).

using input shaping is very certain that there will be a modeling error. Given that there will be a modeling error, there is no reason to force the vibration to be zero at a mode that the system does not have. By relaxing the zero vibration constraint and only requiring that the vibration be at a low level, the EI formulation generates a command signal that is significantly more insensitive to modeling errors than the previously reported input shapers.

A sensitivity curve, which is a plot of the percentage residual vibration [Eq. (11)] as a function of ω, reveals how variations in the system frequency affect the level of residual vibration. Figure 3 compares the sensitivity curve for the EI shaper to the shapers reported previously.

The previously reported shapers were called the time-optimal control and the robust time-optimal control. Given that the EI shaper is more robust than the robust control, we have relabeled the shapers using a more descriptive nomenclature—the shapers are described by the insensitivity constraints they satisfy. The time-optimal control is derived by setting only the residual vibration to zero; therefore, it is labeled the zero vibration (ZV) shaper. The robust control is derived by setting the residual vibration to zero and by setting the derivative of the vibration to zero. Hence, the name zero vibration and zero derivative (ZVD) shaper.

An input shaper's performance in the presence of modeling errors is measured quantitatively by its insensitivity, the width of the sensitivity curve at a specified vibration level.[3] The insensitivity gives us the frequency range over which the vibration is below the desired level.

For the parameter values given with Eq. (16), the 5% insensitivity for the ZV shaper is 0.0533; that is, the residual vibration is less than 5% of the unshaped vibration from 0.9734ω to 1.0267ω ($1.0267 - 0.9734 = 0.0533$). The frequency range is normalized by the nominal frequency ω, so that insensitivity will be nondimensional. The 5% insensitivity for the ZVD shaper is 0.2523. The EI shaper has a 5% insensitivity of 0.3511. This is 40% more insensitive than the ZVD shaper and 660% more insensitive than the ZV shaper.

In general, increasing insensitivity requires increasing command length. The preceding ZV shaper has a command duration of 4.218 s, whereas the ZVD shaper has a duration of 5.866 s. However, the increase in insensitivity obtained by moving from a ZVD to an EI shaper comes with essentially no time penalty (the EI shaper has a duration of 5.902 s).

If even more insensitivity is desired, we can extend the EI concept by designing an input shaper that has two humps in its sensitivity curve, rather than just one. To design this shaper we first specify the shape of the desired sensitivity curve and then solve the equations corresponding to the desired shape. This procedure is a deviation from traditional input shaper design methods, where the constraint equations are formulated first and then the sensitivity curve is used to evaluate the shaper.

Figure 4 shows the shape of the desired sensitivity curve. The constraints that are needed to obtain a solution are labeled on the extremities of the curve as constraints on vibration amplitude [Eq. (11)] and constraints on the derivative of the vibration [Eq. (13)]. When these shape constraints are combined with the impulse amplitude constraints of Eq. (2) and the desired rigid-body constraints of Eqs. (6)

Table 1 Rest-to-rest shaper insensitivity

Shaper	Length, s	5% Insensitivity
ZV	4.2179	0.0533
ZVD	5.8660	0.2523
One-hump EI	5.9019	0.3511
Two-hump EI	7.7709	0.6496

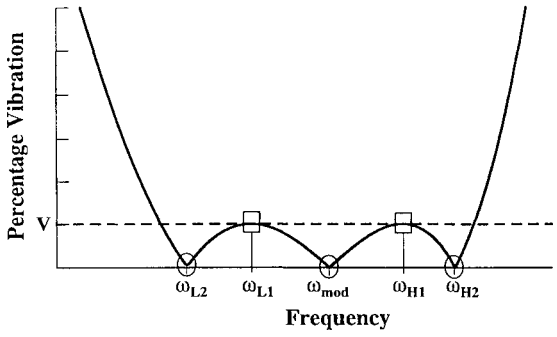

Fig. 4 Desired shape of the sensitivity curve for the two-hump EI shaper: □, set the percentage vibration to V and the derivative of percentage vibration to zero and ○, set the percentage vibration to zero.

and (7), then the set of constraints for the two-hump EI has been completely specified.

The two-hump EI shaper for $V = 0.05$ and $m_1 = m_2 = k = x_d = 1$ is

$$\begin{bmatrix} A_i \\ T_i \end{bmatrix} = \begin{bmatrix} 1 & -2 & 2 & -2 & 2 & -2 & 2 & -2 & 1 \\ 0 & 0.592 & 1.51 & 2.726 & 3.886 & 5.045 & 6.261 & 7.179 & 7.77 \end{bmatrix} \tag{17}$$

The two-hump EI shaper has a 5% insensitivity of 0.6496. This is 260% more insensitive than the ZVD shaper. The significant increase in insensitivity is obtained with a 32% increase in command signal length (7.7709 s as compared with 5.866 s for the ZVD shaper). The insensitivity measures for the preceding shapers are summarized in Table 1.

The EI formulation can be extended to obtain Q humps in the sensitivity curve. For Q even: 1) Set the vibration to 0 at the modeling frequency. 2) Set the vibration equal to V and the derivative equal to 0 at $Q/2$ frequencies higher and $Q/2$ frequencies lower than the modeling frequency. 3) Set the vibration to 0 at $Q/2$ frequencies higher and $Q/2$ frequencies lower than the modeling frequency. 4) The frequencies in steps 2 and 3 must alternate as we move away from the modeling frequency, with a frequency from step 2 occurring first. See Fig. 4.

For Q odd: 1) Set the vibration to V at the modeling frequency. 2) Set the vibration to 0 at $(Q+1)/2$ frequencies higher than the modeling frequency and $(Q+1)/2$ frequencies lower than the modeling frequency. 3) Set the vibration equal to V and the derivative equal to 0 at $(Q-1)/2$ frequencies higher and $(Q-1)/2$ frequencies lower than the modeling frequency. 4) The frequencies in steps 2 and 3 must alternate as we move away from the modeling frequency, with a frequency from step 2 occurring first.

Evaluation of Rest-to-Rest Input Shapers

A computer simulation of the system shown in Fig. 1 was constructed in MATLAB. The simulation was performed using the command signals generated with the rest-to-rest ZVD shaper, $V = 5\%$ one-hump EI shaper, and $V = 5\%$ two-hump EI shaper. Figure 5 compares the system response to the command signals when k, the spring constant, is varied from the nominal value of 1.0–0.6 in steps of −0.1. The frequency changes from 0.225 to 0.174 Hz during this parameter variation. The envelope on the residual vibration from the one-hump EI is only 69% of the vibration from the ZVD shaper. For almost any variation of k, the envelope will be smaller for the

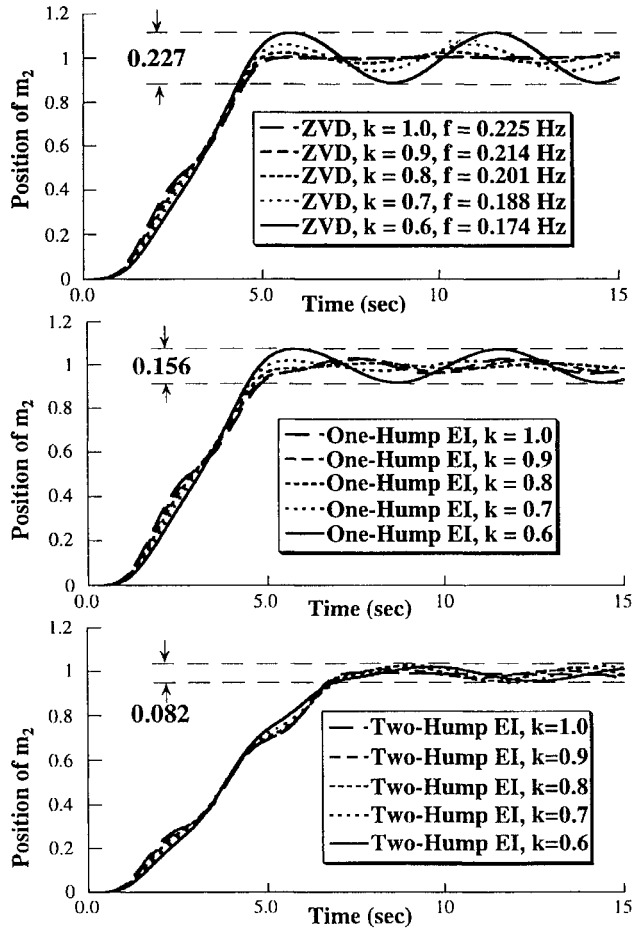

Fig. 5 Comparison of responses to ZVD, EI, and two-hump EI rest-to-rest shapers.

EI shaper. The envelope on the two-hump EI residual vibration is only 36% of the ZVD vibration envelope.

As a further test of the EI input shaper for rest-to-rest slews, we conducted hardware tests on a rotary table. A 24-in. steel beam was mounted to the table surface and a 2-lb mass was attached to the end of the beam. An Inland Torque Motor used to rotate the table was equipped with an HP HEDS-6110 encoder with 44,000 counts per table revolution. The motor was powered by an Aerotech DS16020 amplifier, and the constant-amplitude control signals were generated by a Motion Engineering PC/DSP Motion Controller.

The table was moved with an unshaped command and a fast Fourier transform was performed on the residual vibration. The frequency spectrum showed a dominant low mode at approximately 2 Hz and a second mode close to 8 Hz. For the first test, the 8-Hz mode was neglected. A $V = 5\%$ one-hump EI rest-to-rest shaper was designed for 2 Hz, zero damping, and a 1-rad move. This shaper is

$$\begin{bmatrix} A_i \\ T_i \end{bmatrix} = \begin{bmatrix} 1 & -2 & 2 & -2 & 2 & -2 & 1 \\ 0 & 0.1795 & 0.2388 & 0.4428 & 0.6467 & 0.706 & 0.8855 \end{bmatrix} \tag{18}$$

Figure 6 compares the shaped response and the response to a bang-bang command. The EI shaper reduced the vibration to about 16% of the unshaped vibration level. This is certainly better than not using shaping; however, it is about three times the theoretical level of 5%. The deviation from theory can be largely explained by the presence of the unmodeled 8-Hz vibration, which is clearly visible in Fig. 6.

The problem of the 8-Hz vibration is not surprising if we examine the shaper's sensitivity curve relative to an impulse over a region that includes 8 Hz. (We use the percentage vibration equation relative to an impulse rather than relative to the bang-bang because the

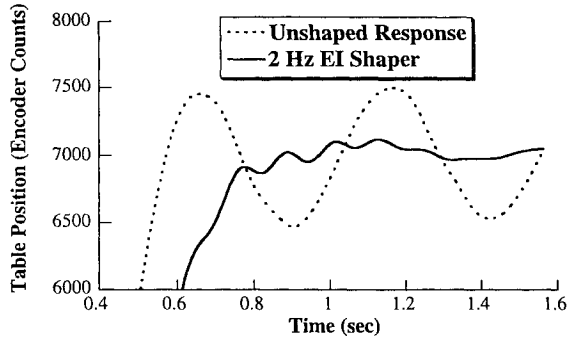

Fig. 6 Experimental unshaped and 2-Hz EI shaped residual vibration.

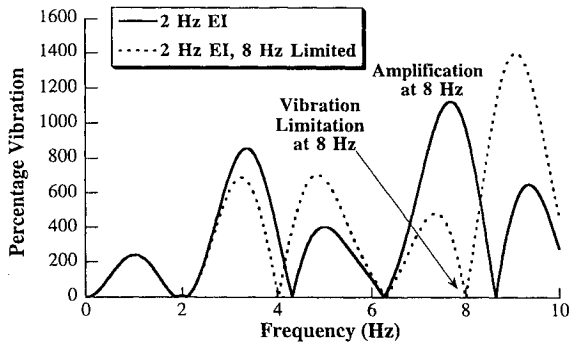

Fig. 7 2-Hz EI shaper and the 2-Hz EI shaper with 8-Hz vibration limitation.

vibration from a bang-bang will go to zero at certain frequencies in the range we are examining. As mentioned earlier, this causes the sensitivity curve relative to the bang-bang to go to infinity at those frequencies.) Figure 7 shows that the shaper will cause an amplification of the 8-Hz mode; the theoretical shaped vibration level at 8 Hz is 10 times more than for an unshaped step.

Elimination of Multiple Vibration Modes

We eliminated the second mode at 8 Hz just as we did the 2-Hz mode, by adding a constraint equation limiting its amplitude. An appropriate constraint equation is a percentage vibration constraint for the second mode:

$$V_2 = \sqrt{[\Sigma A_i \sin(\omega_2 t_i)]^2 + [\Sigma A_i \cos(\omega_2 t_i)]^2} \tag{19}$$

where $\omega_2 = 2\pi^*(8\text{ Hz})$ and $V_2 = 0$. The solution to this augmented set of constraints when $V_2 = 0$ is

$$\begin{bmatrix} A_i \\ T_i \end{bmatrix} = \begin{bmatrix} 1 & -2 & 2 & -2 & 2 & -2 & 2 & -2 & 1 \\ 0 & 0.171 & 0.227 & 0.408 & 0.446 & 0.483 & 0.664 & 0.720 & 0.891 \end{bmatrix} \tag{20}$$

Note that the command length has increased less than 1% to satisfy this multiple mode formulation.

The sensitivity curve for this shaper is compared with the original EI shaper insensitivity in Fig. 7. We did not require insensitivity for the 8-Hz mode because its unshaped amplitude is small compared with the 2-Hz mode.

Figure 8 demonstrates that the 2-Hz EI shaper with the 8-Hz limitation virtually eliminates the high mode from the response. The residual vibration amplitude is now approximately 5.6% of the unshaped level, very close to the theoretical level of 5%.

Input Shaper Design for Acceleration to Constant Velocity

In this section we present input shapers that are designed to accelerate a flexible spacecraft up to a constant slewing velocity using only positive pulses.

Table 2 Positive-pulse shaper insensitivity

Shaper	Length, s	5% Insensitivity
ZV	3.2214	0.0484
ZVD	4.9901	0.2440
One-hump EI	5.0231	0.3400
Two-hump EI	7.0851	0.6413

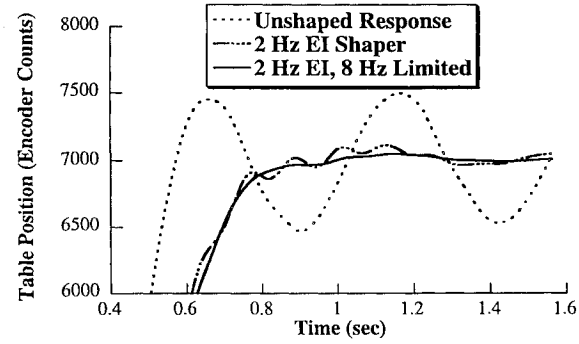

Fig. 8 Removal of the high mode using the 2-Hz EI shaper with the 8-Hz limitation.

In addition to developing the EI shapers, we will present the ZV and ZVD positive-pulse shapers because they have not been presented previously in the literature. The ZV positive-pulse shaper results form solving Eqs. (4), (6), (12), and (15) with $V = 0$. The ZV positive-pulse shaper for $m_1 = m_2 = k = v_d = 1$ is

$$\begin{bmatrix} A_i \\ T_i \end{bmatrix} = \begin{bmatrix} 1 & -1 & 1 & -1 \\ 0 & 1.000 & 2.2214 & 3.2214 \end{bmatrix} \tag{21}$$

This ZV shaper is very sensitive to modeling errors, as was its rest-to-rest counterpart. The ZVD positive-pulse shaper for $m_1 = m_2 = k = v_d = 1$ is

$$\begin{bmatrix} A_i \\ T_i \end{bmatrix} = \begin{bmatrix} 1 & -1 & 1 & -1 & 1 & -1 \\ 0 & 0.4824 & 1.9775 & 3.0127 & 4.5077 & 4.9901 \end{bmatrix} \tag{22}$$

The one- and two-hump EI positive-pulse shapers were also derived using the parameters $m_1 = m_2 = k = v_d = 1$. The one-hump EI positive-pulse shaper is

$$\begin{bmatrix} A_i \\ T_i \end{bmatrix} = \begin{bmatrix} 1 & -1 & 1 & -1 & 1 & -1 \\ 0 & 0.5032 & 2.0147 & 3.0084 & 4.5199 & 5.0231 \end{bmatrix} \tag{23}$$

Once again, the one-hump EI constraints are satisfied with only a negligible increase in command length over the ZVD shaper.

The two-hump EI positive-pulse shaper is

$$\begin{bmatrix} A_i \\ T_i \end{bmatrix} = \begin{bmatrix} 1 & -1 & 1 & -1 & 1 & -1 & 1 & -1 \\ 0 & 0.299 & 2.055 & 2.756 & 4.32 & 5.031 & 6.786 & 7.085 \end{bmatrix} \tag{24}$$

The sensitivity curves relative to a pulse input for all of the preceding positive-pulse shapers are very similar to the curves for their rest-to-rest counterparts shown in Fig. 3. Table 2 summarizes the insensitivity measures for each of the shapers.

We reiterate that positive-pulse shapers do not yield the time-optimal spin-up command. The time-optimal command contains negative force pulses.[22] However, the time-optimal command would probably never be used with real spacecraft because it is very fuel inefficient. The question naturally arises as to how much slower the positive-pulse shapers are than the time-optimal shapers. The time-optimal ZVD shaper for $m_1 = m_2 = k = v_d = 1$ has a length of 4.73 s. The positive-pulse ZVD shaper for the same parameters was given in Eq. (22) and has a length of only 4.99 s. Clearly the

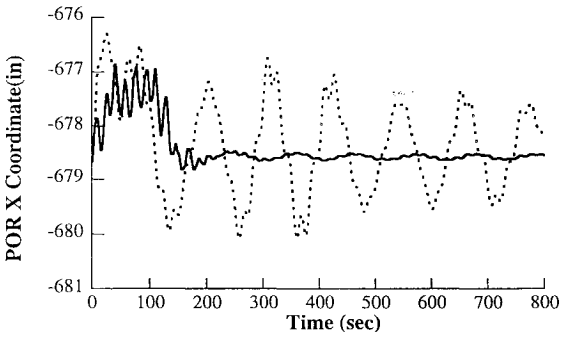

Fig. 9 Oscillations from accelerating the Space Shuttle/space station system: - - - -, single pulse and ——, shaped pulses.

maneuver time is not increased much by eliminating the negative pulses.

To complete the comparison, we calculate the fuel usage for the two types of shapers. The time optimal ZVD shaper uses 4.73 s of fuel (jets are always firing in the positive or negative direction). On the other hand, the positive-pulse ZVD shaper uses only 2.0 s of fuel!

Evaluation of Positive-Pulse Input Shapers

MATLAB simulations using the preceding positive-pulse shapers were performed for $m_1 = m_2 = v_d = 1$ and $1.0 \leq k \leq 0.5$. The envelope on the ZV and ZVD residual vibration is 0.8527 and 0.3878, respectively. The envelope on the one-hump EI shaper is 0.3213. The envelope with the two-hump EI shaper is only 0.0785, but it requires approximately 40% more time to reach the desired velocity than the one-hump EI or the ZVD shaper.

To test the positive-pulse shapers on a complex flexible spacecraft, tests were performed using Draper Laboratory's simulation (the DRS) of the Space Shuttle and its telerobotic manipulator. The DRS was developed over a period of 10 years and has been verified numerous times with actual Space Shuttle flight data. The two simulations performed for this paper included a late 1992 model of the space station attached to the end of the Space Shuttle's remote manipulator.

The goal of the tests was to accelerate the Space Shuttle/space station system up to a constant velocity. The first simulation used was a single jet firing of 38.4 s in duration. The second simulation used a ZVD positive-pulse shaper that reached the same velocity as the single pulse. The shaped pulses were generated for the two most important modes of the system, 0.01 and 0.05 Hz. Figure 9 compares the unshaped and shaped responses of the Space Shuttle simulation. The vibration plotted in Fig. 9 is the point of resolution (POR) X coordinate. The POR is a position vector from the tip of the manipulator to a point fixed in the rigid-body reference frame of the shuttle.

The oscillations in the POR are reduced by an order of magnitude with the shaped pulse profile. The residual vibration that remains is composed of vibration from the 0.01-Hz mode and vibration from less important modes that were not modeled in the shaper design process. The presence of the 0.01-Hz residual is a good argument for using EI shapers. In this case a ZVD shaper was used, but due to the nonlinearity of the model, the 0.01-Hz vibration was not completely eliminated. Given that the vibration cannot be completely eliminated, we should give up the requirement of zero residual vibration (which is unrealistic) and switch to the EI constraints for better robustness.

Conclusions

A technique for designing command profiles for flexible spacecraft equipped with on-off reaction jets has been presented. The technique can design input shapers for rest-to-rest slews or accelerations to constant velocity. The input shapers presented are significantly more robust to modeling errors than similar techniques that have been previously reported. Furthermore, the commands that accelerate to constant velocity are more fuel efficient than profiles designed with related techniques. It was shown that input shapers can be designed by constructing a desired sensitivity curve and then solving the equations obtained from the curve. This procedure is much more intuitive and powerful than the traditional process of formulating constraint equations without consideration of the specific shape of the sensitivity curve. Computer simulations and hardware experiments verified the effectiveness of the control method.

Acknowledgments

Support for this work was provided by Convolve, Inc., under NASA Contract NAS5-32034 and the Office of Naval Research Fellowship Program. We would like to thank Keith Rogers for performing the simulations with the DRS. The methods described in this paper are covered under issued and pending U.S. patents, including 4,916,635; April 10, 1990. Commercial use of these methods requires written permission from the Massachusetts Institute of Technology.

References

[1]Singer, N. C., and Seering, W. P., "Preshaping Command Inputs of Reduce System Vibration," *Journal of Dynamic Systems, Measurement and Control*, Vol. 112, March 1990, pp. 76–82.

[2]Singhose, W., Seering, W., and Singer, N., "Shaping Inputs to Reduce Vibration: A Vector Diagram Approach," *IEEE Conference on Robotics and Automation*, Cincinnati, OH, 1990, pp. 922–927.

[3]Singhose, W., Seering, W., and Singer, N., "Residual Vibration Reduction Using Vector Diagrams to Generate Shaped Inputs," *Journal of Mechanical Design*, Vol. 116, June 1994, pp. 654–659.

[4]Hyde, J. M., and Seering, W. P., "Using Input Command Pre-Shaping to Suppress Multiple Mode Vibration," *IEEE International Conference on Robotics and Automation*, Sacramento, CA, 1991, pp. 2604–2609.

[5]Banerjee, A. K., "Dynamics and Control of the WISP Shuttle-Antennae System" *Journal of Astronautical Sciences*, Vol. 41, No. 1, 1993, pp. 73–90.

[6]Rappole, B. W., Singer, N. C., and Seering, W. P., "Multiple-Mode Impulse Shaping Sequences for Reducing Residual Vibrations," *23rd Biennial Mechanisms Conference*, Minneapolis, MN, DE-Vol. 7, 1994, pp. 11–16.

[7]Jansen, J. F., "Control and Analysis of a Single-Link Flexible Beam with Experimental Verification," Oak Ridge National Lab., ORNL/TM-12198, Dec. 1992.

[8]Magee, D. P., and Book, W. J., "Filtering Schilling Manipulator Commands to Prevent Flexible Structure Vibration," *American Control Conference*, Baltimore, MD, 1994, pp. 2538–2542.

[9]Tzes, A., and Yurkovich, S., "An Adaptive Input Shaping Control Scheme for Vibration Suppression in Slewing Flexible Structures," *IEEE Transactions on Control Systems Technology*, Vol. 1, June 1993, pp. 114–121.

[10]Murphy, B. R., and Watanabe, I., "Digital Shaping Filters for Reducing Machine Vibration," *IEEE Transactions on Robotics and Automation*, Vol. 8, April 1992, pp. 285–289.

[11]Jones, S. D., "Quantification and Reduction of Dynamically Induced Errors in Coordinate Measuring Machines," Ph.D Thesis, Dept. of Mechanical Engineering, Univ. of Michigan, Ann Arbor, MI, 1993.

[12]Seth, N., Rattan, K. S., and Brandstetter, R. W., "Vibration Control of a Coordinate Measuring Machine," *IEEE Conference on Control Applications*, Dayton, OH, 1993, pp. 368–373.

[13]Tuttle, T. D., and Seering, W. P., "A Zero-Placement Technique for Designing Shaped Inputs to Suppress Multiple-Mode Vibration," *American Control Conference*, Baltimore, MD, 1994, pp. 2533–2537.

[14]Rappole, B. W., Singer, N. C., and Seering, W. P., "Input Shaping with Negative Sequences for Reducing Vibrations in Flexible Structures," *American Control Conference*, San Francisco, CA, 1993, pp. 2695–2699.

[15]Singhose, W., Singer, N., and Seering, W., "Design and Implementation of Time-Optimal Negative Input Shapers," ASME International Mechanical Engineering Congress, Chicago, IL, DSC 55-1, 1994, pp. 151–157.

[16]Drapeau, V., and Wang, D., "Verification of a Closed-Loop Shaped-Input Controller for a Five-Bar-Linkage Manipulator," *IEEE International Conference on Robotics and Automation*, Atlanta, GA, 1993, pp. 216–221.

[17]Singhose, W., and Singer, N., "Initial Investigations into the Effects in Input Shaping on Trajectory Following," *American Control Conference*, Baltimore, MD, 1994, pp. 2526–2532.

[18]Rogers, K., "Limiting Vibrations in Systems with Constant Amplitude Actuators Through Command Shaping," Master's Thesis, Dept. of Aeronautics and Astronautics, Massachusetts Inst. of Technology, Cambridge, MA, 1994.

[19]Singhose, W., "A Vector Diagram Approach to Shaping Inputs for Vibration Reduction," Massachusett Inst. of Technology, MIT Artificial Intelligence Lab Memo 1223, Cambridge, MA, March 1990.

[20]Singer, N. C., Seering, W. P., and Pasch, K. A., "Shaping Command Inputs to Minimize Unwanted Dynamics," Massachusetts Inst. of Technology, U.S. Patent 4,916,635, Cambridge, MA, 1990.
[21]Liu, Q., and Wie, B., "Robust Time-Optimal Control of Uncertain Flexible Spacecraft," *Journal of Guidance, Control, and Dynamics*, Vol. 15, No. 3, 1992, pp. 597–604.
[22]Singh, T., and Vadali, S. R., "Robust Time-Optimal Control: A Frequency Domain Approach," *Journal of Guidance, Control, and Dynamics*, Vol. 17, No. 2, 1994, pp. 346–353.
[23]Wie, B., Sinha, R., and Liu, Q., "Robust Time-Optimal Control of Uncertain Structural Dynamic Systems," *Journal of Guidance, Control, and Dynamics*, Vol. 15, No. 5, 1993, pp. 980–983.
[24]Banerjee, A., and Singhose, W., "Slewing and Vibration Control of a Nonlinearity Elastic Shuttle Antenna," AIAA/AAS Astronautics Specialists Conf., Scottsdale, AZ, 1994.
[25]Singhose, W., Bohlke, K., and Seering, W., "Fuel-Efficient Shaped Command Profiles for Flexible Spacecraft," *Proceedings of the AIAA Guidance, Navigation, and Control Conference*, AIAA, Washington, DC, 1995.
[26]Bolz, R. E., and Tuve, G. L., *CRC Handbook of Tables for Applied Engineering Science*, CRC Press, Boca Raton, FL, 1973, p. 1071.
[27]Brooke, A., Kendrick, D., and Meeraus, A., *GAMS: A User's Guide*, Scientific Press, Redwood City, CA, 1988.